Martín-Mateos, P.; Bonilla-Manrique, O.E.; Gutiérrez-Escobero, C. Wavelength modulation laser heterodyne radiometry. In: *Optics Letters,43(12), Jun. 2018, pp. 3009-3012*

DOI: 10.1364/OL.43.003009

Wavelength Modulation Laser Heterodyne Radiometry

PEDRO MARTÍN-MATEOS, OSCAR ELÍAS BONILLA-MANRIQUE AND CRISTINA GUTIÉRREZ-ESCOBERO

Electronics Technology Department, Universidad Carlos III de Madrid, Leganés, 28911 Spain
**Corresponding author: pmmateos@ing.uc3m.es*

Received X March 2018; revised XX Month, XXXX; accepted XX Month XXXX; posted XX Month XXXX (Doc. ID XXXXX); published XX Month XXXX

A novel method is proposed for improving the performance of traditional laser heterodyne radiometry. The technique, which is based on the use of a wavelength modulated local oscillator laser, provides baseline-free spectra, lower limits of detection and better precision and consistency than the conventional approach. This tool could, therefore, boost the accuracy of current terrestrial and planetary atmospheric studies.

OCIS codes: *(120.5630) Radiometry; (280.4788) Optical sensing and sensors; (120.6200) Spectrometers and spectroscopic instrumentation; (300.6310) Spectroscopy, heterodyne.*

http://dx.doi.org/10.1364/OL.99.xxxxx

Laser heterodyne radiometry (LHR) is a well-proven spectral analysis technique that enables exceptionally sensitive optical measurements with ultrahigh spectral resolution [1–5]. Indeed, LHR has paved the way for accurate terrestrial and planetary atmospheric studies operating on both ground-based [6–10] and spaceborne [11] observing infrastructures. This spectral detection method, first demonstrated in the mid-seventies [12,13], is based on heterodyning the incoming optical spectrum with a local oscillator (LO) laser, thus downconverting the optical signal to the radio-frequency (RF) domain. Whereas the subsequent amplification and band-pass filtering of the RF signal (the power of which is eventually detected with a Schottky diode) sets the spectral resolution of the instrument, spectral information is straightforwardly retrieved by sweeping the LO over the wavelength range of interest. Traditionally, in order to boost the sensitivity of LHR instruments, the incoming optical signal is modulated by a chopper unit [1,9], demodulating then the output of the Schottky diode by a lock-in amplifier that is phase-locked to the chopper frequency. Conversely, in this Letter, we analyzed the opportunities offered by the use of a wavelength-modulated LO in an LHR system.

Wavelength modulated laser sources are nowadays the standard approach to active laser-based gas analysis. Wavelength modulation spectroscopy (WMS) [14,15], which is undoubtedly the method of choice for active optical absorption-based gas detection, provides, in fact, much higher sensitivities that direct laser absorption spectroscopy [16]. WMS is founded on the sinusoidal frequency modulation (in addition to the line-sweeping) of the bias current of the laser; the presence of absorption lines within the wavelength range of the system generates in the detector different harmonics of the modulation signal with an amplitude that can be directly related to the concentration of gas (these harmonics are detected by lock-in amplifiers for maximum noise removal). Even though its sensitivity is far higher than that of direct absorption spectroscopy, WMS has as a major drawback the need for calibration. This issue has, nonetheless, been overcome by the development of calibration-free WMS techniques, with several approaches proposed [17–20]. We could argue that the one that has had the greatest impact is the use of the 1f (first harmonic of the modulation frequency) signal to normalize the 2f amplitude for changes in the level of optical power reaching the detector [21–23]. The end result of this procedure is a measurement method that provides calibration-free operation and an improvement in sensitivity of several orders of magnitude over non-modulation methods.

As previously introduced, the aim of this Letter is to present the benefits that a wavelength-modulated LO brings to LHR. The discussion will be structured in different points, as are the comparison between the complexities of the traditional and the new architecture, the spectral waveforms, the existence of baselines and the experimental signal-to-noise ratio (SNR) and precision.

The block diagrams of a traditional and a wavelength-modulated (WM) LHR are shown in Fig. 1 (a) and Fig. 1 (b) respectively. In the traditional scheme, the light entering the system is first modulated and then combined with the LO laser. Both signals are heterodyned on the photodetector resulting on the direct downshifting of the input optical signal to the RF domain. Next, a set of amplifiers and filters control the RF gain and spectral resolution of the instrument and the resulting power is measured by a square law detector. Finally, the output of the RF power detector is demodulated by a lock-in amplifier. Similarly, the architecture of the WM-LHR instrument, shown in Fig. 1 (b), is

practically identical to that of the traditional scheme. The only difference in implementation is that, as the modulation signal is now applied to the laser, the chopper is no longer required. Likewise, in WM-LHR the lock-in amplifier is to be configured to detect also the higher-frequency harmonics of the modulation signal.

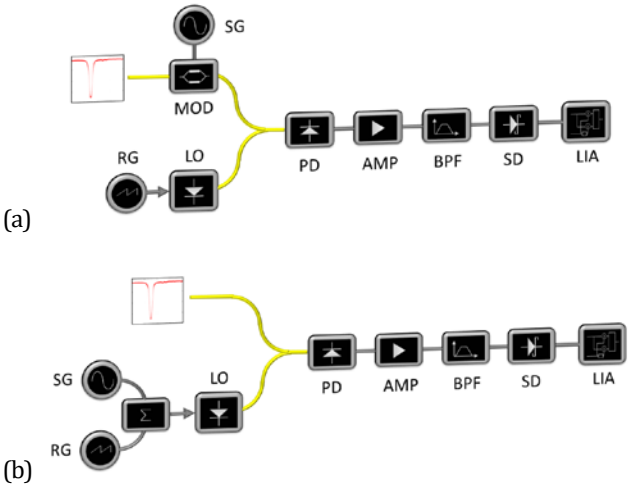

Fig. 1. Block diagrams of (a) a traditional LHR system and (b) a WM-LHR instrument. SG, Signal generator; MOD, Optical chopper; RG, Ramp generator; LO, Local oscillator laser; PD, Photodetector; AMP, RF Amplifier; BPF, Band-pass filter; SD, Schottky detector; LIA, Lock-in amplifier.

The close similarities between the two architectures enable to easily compare the performance of both approaches. Thus, a hybrid system equipping both a chopper and a connection for the intensity modulation of the bias current of the laser was implemented; only one of the modulation systems was employed at a time (according to the desired operation mode). The consistent, well-controlled calibration output of an AQ6370C optical spectrum analyzer (Yokogawa Electric Corp., Japan) was used as light source for the analysis presented in this manuscript (with a power of 250 nW/nm in the range of interest). For the implementation of the setup, a 1542 nm discrete mode laser (Eblana Photonics Ltd., Ireland) was utilized as local oscillator and the modulation of the incoming light was performed using a Lithium Niobate electro-optical intensity modulator (LN56S-FC, Thorlabs Inc., U.S.A.) driven at its half-wave voltage. The optical signals are heterodyned on a battery-powered 150MHz InGaAs photodetector (PDA10CF, Thorlabs Inc., USA), the output of which is amplified by three battery-powered ZFL-500LN (Mini-Circuits Inc., U.S.A.) cascading amplifiers and band-pass filtered between 40 MHz and 150 MHz. This results in a spectral resolution of 300 MHz (0.01 cm^{-1}). The power of the RF signal is then measured by a Schottky detector (EZR0120A3, Eclipse Microwave Inc., U.S.A.) that is finally connected to an HF2LI lock-in amplifier (Zurich Instruments Ltd., Switzerland). The effective integration time of the lock-in amplifier was adjusted to 1 s.

Fig. 2 and Fig. 3 present a comparison of the traditional LHR and the 1f, 2f and 3f WM-LHR experimental signals for the P-27 transition of C_2H_2 at 1542.25 nm (6484.033 cm^{-1}). The characteristic profile of the LHR spectrum, Fig. 2, shows a spectral feature with a base 10 absorbance of approximately 0.019 that includes the typical baseline presented by the technique. In this measurement, the weak absorption of acetylene at 1542.37 nm (6483.529 cm^{-1}) is barely visible, with an amplitude that is close to the noise level of the LHR system. On the contrary, both absorption lines are clearly visible in the 1f WM-LHR spectrum (Fig. 2 (a)). As expected, the obtained waveform resembles that of the classical first harmonic of the WMS method. The two spectral lines are also apparent in Fig. 3 (b), which shows the amplitude of the second harmonic 2f of the WM-LHR signal as a function of wavelength. It is worthwhile noting that the 2f WM-LHR signal is baseline-free, which noticeably simplifies concentration retrieval and increases sensitivity. In the same way, the 3f WM-LHR spectrum, Fig. 3 (c), allows seeing the two molecular transitions without any baseline.

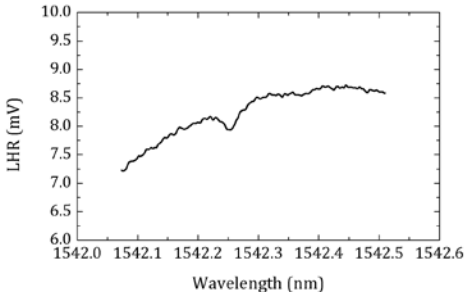

Fig. 2. Traditional LHR output spectrum.

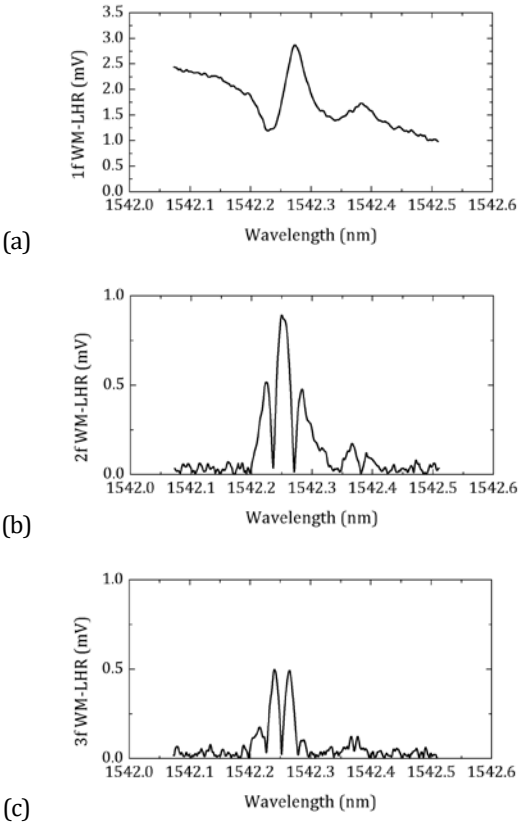

Fig. 3. (a) 1f, (b) 2f, and (c) 3f harmonics of the laser modulation signal in WM-LHR.

To enable a quantitative comparison between the performances of the two different methods, the SNR has been calculated for each of the four measurements previously presented using as a reference the stronger spectral line. In the case of the LHR system, the SNR was obtained as the ratio between the depth of the dip and the standard deviation of the baseline (once fitted) away from the absorption line. Thus, SNRs with an average value of 18.5 are obtained for the classical LHR setup. The SNR of the 1f WM-LHR signal was calculated as the peak-to-valley voltage over, again, the noise in the baseline away from the spectral feature. In the case of the 2f and 3 f WM-LHR harmonics, the SNRs are calculated by dividing the peak voltage by the standard deviation of the noise floor. Average SNRs of 247, 57 and 34 were obtained for the 1f, 2f and 3f WM-LHR measurements respectively, leading to a significant improvement in the sensitivity of the instrument.

The influence of the wavelength modulation amplitude of the laser on the WM-LHR signal was also characterized and the results are shown in Fig. 4. Starting at very low modulation amplitudes, the 2f signal grows as the modulation index increases. Then, the peak 2f value reaches its maximum level before beginning very mildly to fall. The modulation amplitude that maximizes the 2f peak amplitude, found to be 36 pm, was experimentally established in roughly 2 times the full wide at half maximum of the spectral line, which is in very close agreement with the optimum modulation index that can be found in the literature for WMS. All the WM-LHR measurements shown in the manuscript were taken at this optimum modulation amplitude. It should be emphasized that even though the operation at modulation indexes higher than the optimum slightly lessen the 2f peak value, its effect in practice is a significant widening of the spectral features that diminishes the spectral resolution of the radiometer.

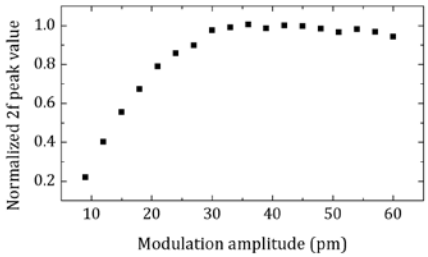

Fig. 4. 2f WM-LHR peak voltage as a function of the modulation index.

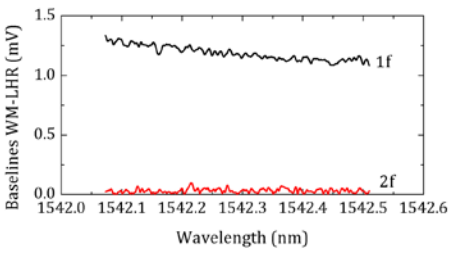

Fig. 5. Baselines of the first (1f) and second (2f) harmonics of WM-LHR when the optical signal is disconnected from the input of the system.

In terms of baseline, the LHR technique has an inherent baseline that depends on the total amount of optical power on both the LO and the input signal. Even though this reference enables calibration-free operation, it limits the sensitivity. In the same way, residual amplitude modulation in the laser makes the baseline of the 1f WM-LHR signal to depend on the incoming optical signal power. By contrast, as referenced above, the 2f and 3f harmonics very conveniently have no baselines. This discussion is graphically illustrated in Fig. 5, where the baselines for the first and second harmonics of the WM-LHR measurement are shown.

As in the case of WMS, the major drawback of WM-LHR is that the amplitudes of the harmonics do not only depend on the strength of the line but also, between other factors, on the total amount of optical power that reaches the instrument. Thus, system calibration to a well-characterized input signal is required for an accurate estimation of the concentration of gas in the atmospheric column. An illustration of this behavior is shown in Fig. 6, in which the peak amplitude of the 2f WM-LHR spectrum is plotted at different power levels.

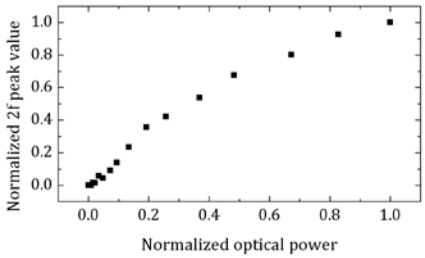

Fig. 6. Normalized 2f WM-LHR peak value for increasing levels of optical power.

As presented in the introduction, several developments have, nevertheless, addressed this disadvantage on WMS, enabling calibration-free operation. One of the most important steps in the process was realizing that the 1f signal can be employed to normalize the amplitude of the higher harmonics for variations in the input intensity [22,23]. The WM-LHR system presented in this Letter has also demonstrated this feature. An additional experiment was carried out in which the level of optical power delivered to the instrument was controlled by a fiber-connectorized optical attenuator. Thus, whereas the 1f and 2f harmonic signals were simultaneously measured by the lock-in amplifier, the level of input power was varied by two orders of magnitude. Fig. 7 shows the ratio of the 2f signal peak divided by the baseline-compensated 1f offset value at the location of the 2f peak calculated from the previous set of measurements. As can be clearly seen, the 2f/1f ratio is independent of the level of optical power at the input of the system; indeed the dispersion of the values of the 2f/1f ratio is only noticeably increased when the power at the input of the system approaches the noise floor of the instrument. Within the power range at which the system operates with sufficient SNR (normalized power above 0.15), the standard deviation of the 2f/1f ratio over its mean results in a value of 2.8 %, which implies a twofold improvement over the SNR that the traditional LHR method can provide at maximum input power. It seems reasonable to assume that future developments of WM-LHR could further improve the performance of the method by the use of more elaborate calibration-free approximations.

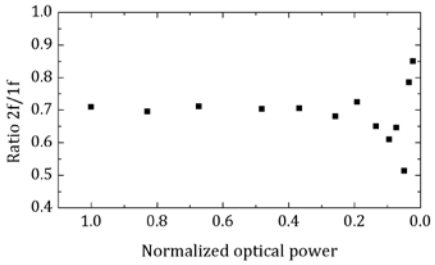

Fig. 7. Ratio of the 2f signal peak divided by the baseline-compensated 1f amplitude at the location of the 2f peak as a function of the normalized optical power at the input of the instrument.

The precisions of the WM-LHR and LHR systems were also evaluated by performing 12 successive spectral measurements at 5 minutes intervals. In the case of WM-LHR, the standard deviation of the 2f/1f ratio over its mean was characterized throughout the whole analysis period resulting in a precision of 1.85 %. The spectroscopic precision of the LHR system (average standard deviation of the peak value divided by the line absorption) for the same input signal and under the same experimental conditions was found to be 4.75 %. The results of this final comparative assessment confirm that WM-LHR is a method that can potentially provide not only an enhanced limit of detection but also better consistency and accuracy in the quantification of atmospheric constituents.

In conclusion, in this Letter, we have investigated the features of an LHR instrument with a wavelength modulated LO. Wavelength modulated optical sources are nowadays the common approach to sensitive active optical gas detection; nevertheless, this technology has not been adopted by optical radiometry yet. Opportunely, the WM-LHR architecture is very similar to the traditional LHR scheme; basically, the modulator (chopper) at the optical input is replaced by an additional sinusoidal modulation of the LO laser in the WM-LHR system. This change brings the immediate advantage of reduced insertion losses at the input of the instrument, what could be directly reflected in an enhancement of the SNR of the system. It must be stressed then that the adaptation of a traditional LHR setup to WM-LHR operation is straightforward.

In the experimental comparison of performance presented in the Letter, a hybrid system was implemented for the analysis of the spectral features of C_2H_2 at 1542.25 nm and 1542.37 nm, being the second line much weaker than the first transition. This setup is an ideal platform for the comparative evaluation of both approaches given that the input optical chopper and the LO modulation signal can be promptly commuted to enable traditional or WM operation modes. A first look of the LHR and 1f, 2f, and 3f WM-LHR spectra confirmed that whereas the weaker resonance of the pair is clearly visible in the three WM-LHR signals at a first glance, it is difficult to identify it in the measurement of the spectrum of the traditional LHR system. This preliminary visual assessment is confirmed by the experimental SNRs obtained; demonstrating that, in the same operating conditions, the first harmonic of the WM-LHR system can improve by more than an order magnitude the SNR of a traditional LHR setup. As a matter of fact, in all the cases that were analyzed, the WM-LHR harmonics presented an SNR superior to that of LHR. It was also demonstrated that in WM-LHR, as in WMS, there is an optimum modulation amplitude for the LO that maximized the peak voltages of the different harmonics. Baselines were also studied, demonstrating how whereas the residual amplitude modulation of the laser creates a noticeable baseline in the 1f WM-LHR; a zero-baseline signal is obtained for the higher order harmonics.

Arguably the strongest drawback of WM-LHR is that, as expected, the amplitudes of all the harmonics depend on the total amount of power that reaches the instrument. Nevertheless, the experimental tests performed confirmed that the ratio between the 2f peak amplitude and the 1f offset level at the location of the 2f peak is constant within an input power range close to two orders of magnitude (limited by the noise floor of the instrument). An obtained dispersion in the value of the ratio of 2.8 % for an input power range of almost an octave demonstrates that WM-LHR provides a superior line-calibrated SNR than that yielded by LHR (even when characterized at higher input power levels). In the same way, WM-LHR has also demonstrated a better precision and concentration-retrieval stability for the repeated characterization of spectral signals. In view of the previous results, it seems reasonable to assume that WM-LHR may open the possibility of future heterodyne radiometers with the ability to improve the sensitivity, the accuracy and the consistency of current systems and, hence, of unlocking new opportunities for terrestrial and planetary atmospheric exploration.

References

1. D. Weidmann, T. Tsai, N. a Macleod, and G. Wysocki, Opt. Lett. **36**, 1951 (2011).
2. G. Sonnabend, D. Wirtz, and R. Schieder, Appl. Opt. **44**, 7170 (2005).
3. D. Stupar, J. Krieg, P. Krötz, G. Sonnabend, M. Sornig, T. F. Giesen, and R. Schieder, Appl. Opt. **47**, 2993 (2008).
4. D. Weidmann and G. Wysocki, Opt. Express **17**, 248 (2009).
5. T. Stangier, G. Sonnabend, and M. Sornig, Remote Sens. **5**, 3397 (2013).
6. H. Nakagawa, S. Aoki, H. Sagawa, Y. Kasaba, I. Murata, G. Sonnabend, M. Sornig, S. Okano, J. R. Kuhn, J. M. Ritter, M. Kagitani, T. Sakanoi, M. Taguchi, and K. Takami, Planet. Space Sci. **126**, 34 (2016).
7. T. Stangier, T. Hewagama, M. Sornig, G. Sonnabend, T. Kostiuk, M. Herrmann, and T. Livengood, Planet. Space Sci. **113–114**, 359 (2015).
8. E. L. Wilson, M. L. McLinden, J. H. Miller, G. R. Allan, L. E. Ott, H. R. Melroy, and G. B. Clarke, Appl. Phys. B **114**, 385 (2014).
9. H. R. Melroy, E. L. Wilson, G. B. Clarke, L. E. Ott, J. Mao, A. K. Ramanathan, and M. L. McLinden, Appl. Phys. B Lasers Opt. **120**, 609 (2015).
10. A. Hoffmann, N. A. Macleod, M. Huebner, and D. Weidmann, Atmos. Meas. Tech. **9**, 5975 (2016).
11. D. Weidmann, A. Hoffmann, N. Macleod, K. Middleton, J. Kurtz, S. Barraclough, and D. Griffin, Remote Sens. **9**, 1073 (2017).
12. R. T. Menzies, Appl. Phys. Lett. **22**, 592 (1973).
13. R. T. Menzies and M. S. Shumate, Science **184**, 570 (1974).
14. J. A. Silver, Appl. Opt. **31**, 707 (1992).
15. D. S. Bomse, A. C. Stanton, and J. A. Silver, Appl. Opt. **31**, 718 (1992).
16. P. Werle, R. Mücke, and F. Slemr, Appl. Phys. B Photophysics Laser Chem. **57**, 131 (1993).
17. J. Chen, A. Hangauer, R. Strzoda, and M.C. Amann, Appl. Phys. B **102**, 381 (2011).
18. J. R. P. Bain, W. Johnstone, K. Ruxton, G. Stewart, M. Lengden, and K. Duffin, J. Light. Technol. **29**, 987 (2011).
19. G. Zhao, W. Tan, J. Hou, X. Qiu, W. Ma, Z. Li, L. Dong, L. Zhang, W. Yin, L. Xiao, O. Axner, and S. Jia, Opt. Express **24**, 1723 (2016).
20. J. Henningsen and H. Simonsen, Appl. Phys. B Lasers Opt. **70**, 627 (2000).
21. H. Li, G. B. Rieker, X. Liu, J. B. Jeffries, and R. K. Hanson, Appl. Opt. **45**, 1052 (2006).
22. G. B. Rieker, J. B. Jeffries, and R. K. Hanson, Appl. Opt. **48**, 5546 (2009).
23. D. T. Cassidy and J. Reid, Appl. Opt. **21**, 1185 (1982).

Full References

1. D. Weidmann, T. Tsai, N. a Macleod, and G. Wysocki, "Atmospheric observations of multiple molecular species using ultra-high-resolution external cavity quantum cascade laser heterodyne radiometry," Opt. Lett. **36**, 1951–1953 (2011).

2. G. Sonnabend, D. Wirtz, and R. Schieder, "Evaluation of quantum-cascade lasers as local oscillators for infrared heterodyne spectroscopy.," Appl. Opt. **44**, 7170–7172 (2005).

3. D. Stupar, J. Krieg, P. Krötz, G. Sonnabend, M. Sornig, T. F. Giesen, and R. Schieder, "Fully reflective external-cavity setup for quantum-cascade lasers as a local oscillator in mid-infrared wavelength heterodyne spectroscopy.," Appl. Opt. **47**, 2993–2997 (2008).

4. D. Weidmann and G. Wysocki, "High-resolution broadband (>100 cm^{-1}) infrared heterodyne spectro-radiometry using an external cavity quantum cascade laser.," Opt. Express **17**, 248–259 (2009).

5. T. Stangier, G. Sonnabend, and M. Sornig, "Compact setup of a tunable heterodyne spectrometer for infrared observations of atmospheric trace-gases," Remote Sens. **5**, 3397–3414 (2013).

6. H. Nakagawa, S. Aoki, H. Sagawa, Y. Kasaba, I. Murata, G. Sonnabend, M. Sornig, S. Okano, J. R. Kuhn, J. M. Ritter, M. Kagitani, T. Sakanoi, M. Taguchi, and K. Takami, "IR heterodyne spectrometer MILAHI for continuous monitoring observatory of Martian and Venusian atmospheres at Mt. Haleakalā, Hawaii," Planet. Space Sci. **126**, 34–48 (2016).

7. T. Stangier, T. Hewagama, M. Sornig, G. Sonnabend, T. Kostiuk, M. Herrmann, and T. Livengood, "Thermal structure of Venus' nightside mesosphere as observed by infrared heterodyne spectroscopy at 10 µm," Planet. Space Sci. **113**–**114**, 359–368 (2015).

8. E. L. Wilson, M. L. McLinden, J. H. Miller, G. R. Allan, L. E. Ott, H. R. Melroy, and G. B. Clarke, "Miniaturized laser heterodyne radiometer for measurements of CO_2 in the atmospheric column," Appl. Phys. B **114**, 385–393 (2014).

9. H. R. Melroy, E. L. Wilson, G. B. Clarke, L. E. Ott, J. Mao, A. K. Ramanathan, and M. L. McLinden, "Autonomous field measurements of CO_2 in the atmospheric column with the miniaturized laser heterodyne radiometer (Mini-LHR)," Appl. Phys. B Lasers Opt. **120**, 609–615 (2015).

10. A. Hoffmann, N. A. Macleod, M. Huebner, and D. Weidmann, "Thermal infrared laser heterodyne spectroradiometry for solar occultation atmospheric CO_2 measurements," Atmos. Meas. Tech. **9**, 5975–5996 (2016).

11. D. Weidmann, A. Hoffmann, N. Macleod, K. Middleton, J. Kurtz, S. Barraclough, and D. Griffin, "The Methane Isotopologues by Solar Occultation (MISO) Nanosatellite Mission: Spectral Channel Optimization and Early Performance Analysis," Remote Sens. **9**, 1073 (2017).

12. R. T. Menzies, "Remote detection of SO_2 and CO_2 with a heterodyne radiometer," Appl. Phys. Lett. **22**, 592–593 (1973).

13. R. T. Menzies and M. S. Shumate, "Air Pollution: Remote Detection of Several Pollutant Gases with a Laser Heterodyne Radiometer," Science **184**, 570–572 (1974).

14. J. A. Silver, "Frequency-modulation spectroscopy for trace species detection: theory and comparison among experimental methods.," Appl. Opt. **31**, 707–717 (1992).

15. D. S. Bomse, A. C. Stanton, and J. A. Silver, "Frequency modulation and wavelength modulation spectroscopies: comparison of experimental methods using a lead-salt diode laser," Appl. Opt. **31**, 718–731 (1992).

16. P. Werle, R. Mücke, and F. Slemr, "The limits of signal averaging in atmospheric trace-gas monitoring by tunable diode-laser absorption spectroscopy (TDLAS)," Appl. Phys. B Photophysics Laser Chem. **57**, 131–139 (1993).

17. J. Chen, A. Hangauer, R. Strzoda, and M.C. Amann, "VCSEL-based calibration-free carbon monoxide sensor at 2.3 µm with in-line reference cell," Appl. Phys. B **102**, 381–389 (2011).

18. J. R. P. Bain, W. Johnstone, K. Ruxton, G. Stewart, M. Lengden, and K. Duffin, "Recovery of Absolute Gas Absorption Line Shapes Using Tunable Diode Laser Spectroscopy With Wavelength Modulation—Part 2: Experimental Investigation," J. Light. Technol. **29**, 987–996 (2011).

19. G. Zhao, W. Tan, J. Hou, X. Qiu, W. Ma, Z. Li, L. Dong, L. Zhang, W. Yin, L. Xiao, O. Axner, and S. Jia, "Calibration-free wavelength-modulation spectroscopy based on a swiftly determined wavelength-modulation frequency response function of a DFB laser," Opt. Express **24**, 1723–1733 (2016).

20. J. Henningsen and H. Simonsen, "Quantitative wavelength-modulation spectroscopy without certified gas mixtures," Appl. Phys. B Lasers Opt. **70**, 627–633 (2000).

21. H. Li, G. B. Rieker, X. Liu, J. B. Jeffries, and R. K. Hanson, "Extension of wavelength-modulation spectroscopy to large modulation depth for diode laser absorption measurements in high-pressure gases.," Appl. Opt. **45**, 1052–1061 (2006).

22. G. B. Rieker, J. B. Jeffries, and R. K. Hanson, "Calibration-free wavelength-modulation spectroscopy for measurements of gas temperature and concentration in harsh environments.," Appl. Opt. **48**, 5546–5560 (2009).

23. D. T. Cassidy and J. Reid, "Atmospheric pressure monitoring of trace gases using tunable diode lasers.," Appl. Opt. **21**, 1185–1190 (1982).